Eur. Phys. J. A **41**, 7–11 (2009)
DOI 10.1140/epja/i2009-10801-y

THE EUROPEAN PHYSICAL JOURNAL A

Letter

Improved bounds on the radius and curvature of the $K\pi$ scalar form factor and implications to low-energy theorems

Gauhar Abbas[a] and B. Ananthanarayan[b]

Centre for High Energy Physics, Indian Institute of Science, Bangalore 560 012, India

Received: 11 March 2009 / Revised: 26 April 2009
Published online: 24 May 2009 – © Società Italiana di Fisica / Springer-Verlag 2009
Communicated by J. Bijnens

Abstract. We obtain stringent bounds in the $\langle r^2\rangle_S^{K\pi}$-$c$ plane where these are the scalar radius and the curvature parameters of the scalar $K\pi$ form factor, respectively, using analyticity and dispersion relation constraints, the knowledge of the form factor from the well-known Callan-Treiman point $m_K^2 - m_\pi^2$, as well as at $m_\pi^2 - m_K^2$, which we call the second Callan-Treiman point. The central values of these parameters from a recent determination are accomodated in the allowed region provided the higher loop corrections to the value of the form factor at the second Callan-Treiman point reduce the one-loop result by about 3% with $F_K/F_\pi = 1.21$. Such a variation in magnitude at the second Callan-Treiman point yields $0.12\,\mathrm{fm}^2 \lesssim \langle r^2\rangle_S^{K\pi} \lesssim 0.21\,\mathrm{fm}^2$ and $0.56\,\mathrm{GeV}^{-4} \lesssim c \lesssim 1.47\,\mathrm{GeV}^{-4}$ and a strong correlation between them. A smaller value of F_K/F_π shifts both bounds to lower values.

PACS. 11.55.Fv Dispersion relations – 12.39.Fe Chiral Lagrangians

The scalar $K\pi$ form factor $f_0(t)$, where t is the square of the momentum transfer, is of fundamental importance in semi-leptonic decays of the kaon and has been studied in great detail, see, *e.g.* [1] for a recent review. In chiral perturbation theory it was computed to one-loop accuracy in ref. [2] and to two-loop accuracy in refs. [3,4]. It has a branch cut starting at the threshold $t_+ = (m_K + m_\pi)^2$ and is analytic elsewhere in the complex plane. The scalar radius $\langle r^2\rangle_S^{K\pi}$ and the curvature parameter c arise in the expansion

$$f_0(t) = f_+(0)\left(1 + \frac{1}{6}\langle r^2\rangle_S^{K\pi} t + ct^2 + \ldots\right), \qquad (1)$$

where $f_+(t)$ is the corresponding vector form factor which here we normalize to 0.976 as in a recent important work [5] that we use for comparison with our results. An important result on this form factor concerns its value at the unphysical point $(m_K^2 - m_\pi^2)$, known as the Callan-Treiman (CT) point [6] (see also ref. [7]) and here it equals $F_K/F_\pi \simeq 1.21$[1], the ratio of the kaon and pion decay constants resulting from a soft-pion theorem. It receives very small corrections at one-loop order which are expected to stay small at higher orders as well (for recent discussions, see refs. [8,9]; note that in this work we are in the isospin conserving limit). These involve coupling constants C_{12}^r and C_{34}^r for which there are estimates in the literature [4,10], and whose consequences have been discussed at length in a recent paper [11]. A soft-kaon analogue fixes its value at tree level at $m_\pi^2 - m_K^2$ (which we will refer to as the second CT point) to be F_π/F_K [12]. The one-loop correction, $\tilde{\Delta}_{CT}^{NLO}$, increases the value by 0.03 [2]. The rather small size of this correction may be traced to the fact that it is parameter free at this level. The corresponding correction at two-loop level has been estimated, which gives the estimate $-0.035 < \tilde{\Delta}_{CT}^{NNLO} < 0.11$ [11]. One of the important findings in our work is that this correction can actually be estimated using analyticity methods and substantially restricts the range above, while remaining consistent with it.

Bourrely and Caprini (BC) [13] consider certain dispersion relations for observables denoted by $\Psi''(Q^2)$ and $(\Psi(Q^2)/Q^2)' + \Psi(0)/Q^4$ (which we will name $\mathcal{O}_1$ and $\mathcal{O}_2$, respectively) involving the square of the form factor. Employing the information at the first CT point and phase of the form factor along the cut they obtained bounds on the scalar radius and curvature parameters. (For an accessible introduction to the methods involved, see ref. [14].) Our work inspired by BC, will use the information at both the CT points to constrain the expansion coefficients using the same observables, but will not include the phase information. We will find that in order to accomodate well-known

[a] e-mail: gabbas@cts.iisc.ernet.in
[b] e-mail: anant@cts.iisc.ernet.in

[1] Although now a little too large, we mainly adopt this value in order to compare our results with prior results.

determinations of the same coefficients [5], the value of the scalar form factor at the second CT point would have to be lowered by about 3% compared to its one-loop value. This is consistent with the estimate given in ref. [11], and significantly pins down the correction. In addition, we consider the observable $\Pi'(Q^2)$ studied by Caprini [15] which we denote by $\mathcal{O}_3$.

To begin, one introduces a conformal variable z,

$$z(t) = S\left(\frac{\sqrt{t_+} - \sqrt{t_+ - t}}{\sqrt{t_+} + \sqrt{t_+ - t}}\right), \tag{2}$$

where S can be ± 1 depending on the convention (the convention of BC corresponds to $S = +1$, while that of ref. [15] corresponds to $S = -1$). The relevant dispersion relation is brought into a canonical form:

$$\frac{1}{2\pi}\int_{-\pi}^{\pi} \mathrm{d}\theta |h(\exp(i\theta))|^2 \leq I, \tag{3}$$

where I is the bound and is associated with the observable in question. In the above, we have

$$h(z) = f(z)w(z), \tag{4}$$

where $f(z)$ is the form factor in terms of the conformal variable and $w(z)$ is the outer function associated with the relevant dispersion relation and the Jacobian of the transformation from t to $z(\equiv \exp(i\theta))$. The function $h(z)$ then admits an expansion given by

$$h(z) = a_0 + a_1 z + a_2 z^2 + \ldots, \tag{5}$$

where the a_i are real. From the Parseval theorem of Fourier analysis, we have $a_0^2 + a_1^2 + a_2^2 + \ldots \leq I$. Improvements on the bound result from additional information which may be at values of 1) space-like momenta, or 2) time-like momenta below threshold, where the form factor is real, or 3) at time-like momenta above threshold, where one may have knowledge either of the modulus or the phase or both. Alternatively, if I is known, and the series is truncated, then one may obtain bounds on the allowed values of the expansion coefficients of the form factor. In BC, the value of the form factor at the first CT point which belongs to the category 2) above, and the phase of the form factor between threshold and $1\,\mathrm{GeV}^2$ in the region of the type 3) above have been used. The improvements result when one takes the constraints one at a time, and further when they are simultaneously imposed. In BC the significant constraint is that from the CT point, in relation to the constraint from the phase of the form factor. In the present work the result of wiring in the second CT constraint alone, and simultaneously with the first one are studied. We will consider the three observables $\mathcal{O}_1$, $\mathcal{O}_2$ and $\mathcal{O}_3$. Their corresponding outer functions are listed in the appendix. Next, we need to consider the

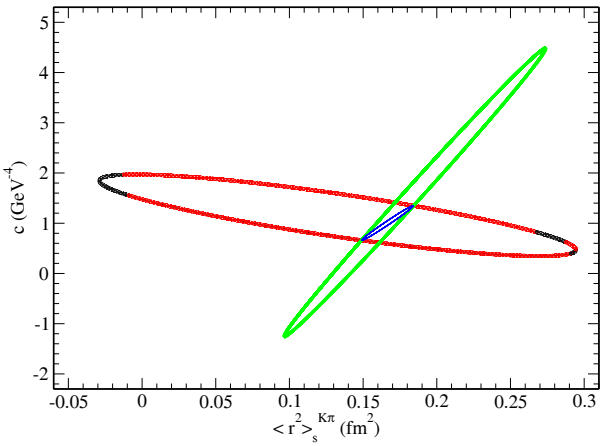

Fig. 1. Boundaries of the allowed regions in the $\langle r^2\rangle_S^{K\pi}$-$c$ plane The flat ellipse comes from the constraint at the first CT point (see also [13]), the long narrow ellipse from the constraint at the second CT point. The small ellipse results from simultaneous inclusion of both constraints.

following expansion coefficients:

$$a_0 = h(0) = f_+(0)w(0), \tag{6}$$

$$a_1 = h'(0) = f_+(0)\left(w'(0) + S\frac{2}{3}\langle r^2\rangle_S^{K\pi} t_+ w(0)\right), \tag{7}$$

$$a_2 = \frac{h''(0)}{2!} = \frac{f_+(0)}{2}\left[w(0)\left(-\frac{8}{3}\langle r^2\rangle_S^{K\pi} t_+ + 32\,c\,t_+^2\right)\right] + \frac{f_+(0)}{2}\left[2w'(0)\left(S\frac{2}{3}\langle r^2\rangle_S^{K\pi} t_+\right) + w''(0)\right]. \tag{8}$$

Improving the bounds on expansion coefficients subject to constraints from the space-like region has been studied recently in the context of the pion electromagnetic form factor [16]. The results there are also applicable to the case at hand: our bounds are obtained by solving the determinantal equation for an observable which in general reads:

$$\begin{vmatrix} I & a_0 & a_1 & a_2 & h(x_1) & h(x_2) \\ a_0 & 1 & 0 & 0 & 1 & 1 \\ a_1 & 0 & 1 & 0 & x_1 & x_2 \\ a_2 & 0 & 0 & 1 & x_1^2 & x_2^2 \\ h(x_1) & 1 & x_1 & x_1^2 & (1-x_1^2)^{-1} & (1-x_1x_2)^{-1} \\ h(x_2) & 1 & x_2 & x_2^2 & (1-x_2x_1)^{-1} & (1-x_2^2)^{-1} \end{vmatrix} = 0, \tag{9}$$

where x_1 and x_2 are the values of z corresponding to $t = m_K^2 - m_\pi^2$ and $t = m_\pi^2 - m_K^2$, respectively, and have the numerical values $x_1 = S \times 0.202$, $x_2 = S \times (-0.111)$. In the above, observable by observable, we input values for the quantity I. Discarding both the rows and columns corresponding to x_1 and x_2 would give the bounds with no constraints, discarding the row and column corresponding to x_1 would amount to including the constraint from only x_2 and *vice versa*. The results of our analysis are displayed in figs. 1–4 and in the discussion below. For these purposes the value of the form factor at the first CT point

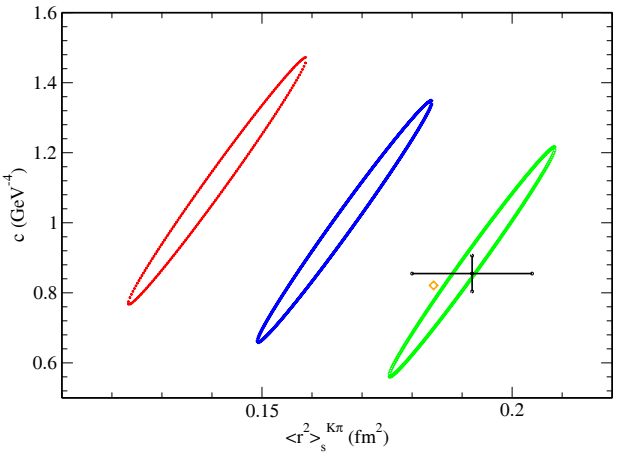

Fig. 2. Allowed ellipses when the value of the scalar form factor at the second CT point is changed from the one-loop result. The higher ellipse is for an increase in its value by 3%, the central ellipse is for when it is not changed, and the lower ellipse is for when it is lowered by 3%. Also marked are the best values from ref. [5], following [13], which essentially lie in the lowest ellipse.

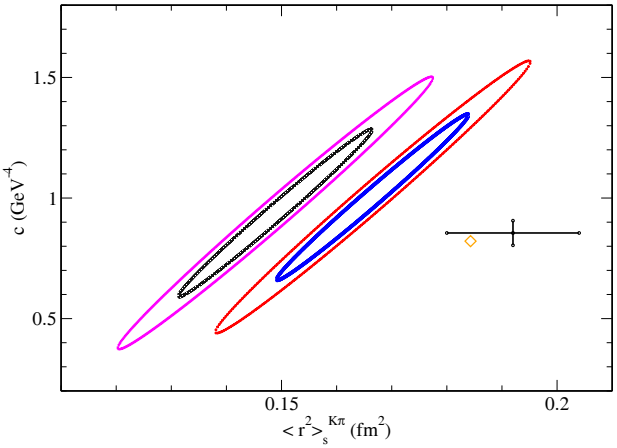

Fig. 3. The ellipses for choices for different input values of I_1. The inner ellipse is for the choice from ref. [17], while the outer ellipse for the choice from ref. [18], and for choices of F_K/F_π of 1.19 and 1.21. The set of ellipses to the left correspond to the former while those to the right to the latter. Also marked are the best values from ref. [5], following [13].

is always taken to be the ratio F_K/F_π, while at the second CT point it is taken to be at its one-loop value of $F_\pi/F_K + 0.03$, unless otherwise mentioned. Unless otherwise mentioned F_K/F_π is taken to be 1.21 in order to carry out a meaningful comparison with the results of BC.

In fig. 1, we display the result obtained when the observable $\mathcal{O}_1$ is used. We use as an input for I_1 the number 0.000079 as in ref. [13], obtained from perturbative QCD with the choice $Q^2 = 4\,\mathrm{GeV}^2$, and choice of masses as given in ref. [17]. The result of including the constraint from the second CT point is truly dramatic isolating a significantly different region (the major axes of the two large ellipses are essentially orthogonal). This feature is

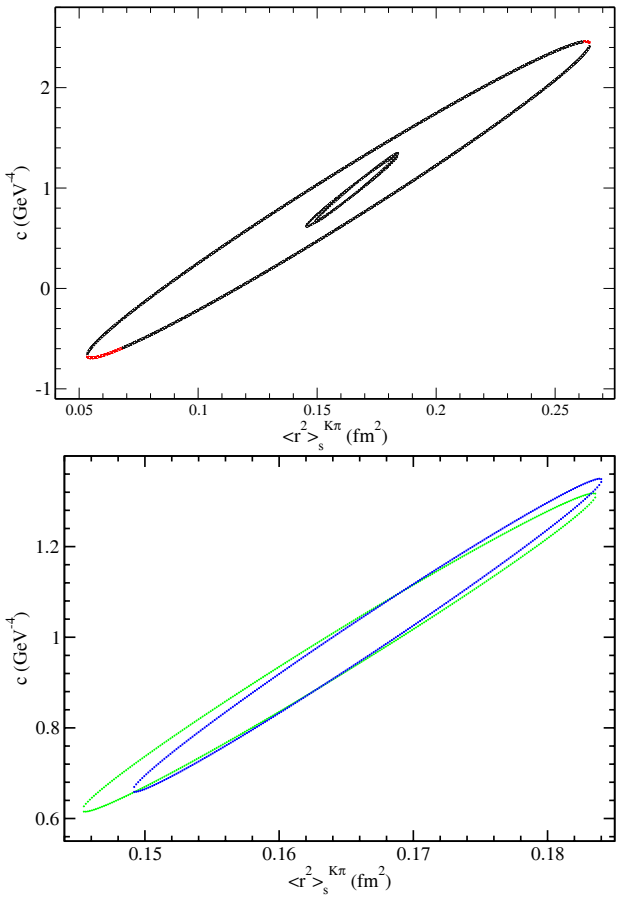

Fig. 4. Allowed regions shown for different choices of input observables. In the top panel, the large ellipse is the allowed region from the observable $\mathcal{O}_3$. Of the two smaller ones, the ellipse that is higher at the right extremity is for the observable $\mathcal{O}_1$, while the other is for $\mathcal{O}_2$ (the lower panel zooms into the region of the latter two ellipses).

special to this system where one constraint comes from the time-like yet unphysical region (first CT point) while the other from a genuine space-like region (second CT point). Taking the contraints one at a time leads to a small region of intersection and the ellipse obtained with simultaneous inclusion is even smaller. For this case we find the range to be $0.15\,\mathrm{fm}^2 \lesssim \langle r^2\rangle_S^{K\pi} \lesssim 0.19\,\mathrm{fm}^2$ and $0.65\,\mathrm{GeV}^{-4} \lesssim c \lesssim 1.35\,\mathrm{GeV}^{-4}$, and we have the approximate relation $c \simeq 19.4\langle r^2\rangle_S^{K\pi} - 2.2$ which is the equation of the major axis of the ellipse, where $\langle r^2\rangle_S^{K\pi}$ is in fm^2 and c is in GeV^{-4}. As such, it would therefore imply that the curvature effects are not negligible and must be included in fits to experimental data, as already observed in, *e.g.*, refs. [13,1]. We have checked that the ellipse has a non-trivial intersection with the band determined by the dispersive representation relation between the slope and curvature parameters given in eq. (2.11) of ref. [1].

The system is sensitive to the value of the form factors at the CT points. Since its value at the first CT point is expected to be stable, we hold it fixed and consider the variation at the second CT point only. Although not entirely consistent as the corrections at both are correlated

in chiral perturbation theory, this is done for purposes of illustration. In fig. 2, we display the effect of varying the value of the scalar form factor at the second CT point in a 3% range compared to its one-loop value. Also shown in this figure are the results of a recent evaluation of the two quantities of interest [5] in the form a diamond and a cross, following the discussion of BC. As the one-loop value is lowered by 3%, these are essentially accomodated in the ellipse, which we consider to be remarkable.

We display in fig. 3 the results obtained by changing 1) the input to the observable, and 2) the value of F_K/F_π which is taken to be 1.21, as before, and 1.19, as a test of sensitivity to the inputs. For the former, we follow BC [13]: we consider changing the value of the input I_1 to the value 0.00020 corresponding to the choice of quark masses from ref. [18]. This choice continues to be reasonable as a recent determination of quark masses [19] yields quark masses numbers that lie between those of the two prior determinations cited above. It may be observed that for F_K/F_π of 1.21, even the larger ellipse does not accomodate the diamond and cross. We now have $0.14\,\mathrm{fm}^2 \lesssim \langle r^2\rangle_S^{K\pi} \lesssim 0.20\,\mathrm{fm}^2$ and $0.43\,\mathrm{GeV}^{-4} \lesssim c \lesssim 1.58\,\mathrm{GeV}^{-4}$.

We test our constraints by changing the observables: as in BC, the first and second observables are both evaluated with the MILC data [17], and we take for the input of the second observable, I_2, the value 0.00022, evaluated at $Q^2 = 4\,\mathrm{GeV}^2$. The observable $\mathcal{O}_3$ has to be adapted to the problem at hand: following Caprini, ref. [15], we take I_3 to be $0.0133\,\mathrm{GeV}^{-2}/(m_K^2 - m_\pi^2)^2$ with $Q^2 = 2\,\mathrm{GeV}^2$. $\mathcal{O}_3$ provides a much larger allowed region as it is not optimal for the problem at hand; the original observable brings in the vector form factor as well. The observables $\mathcal{O}_1$ and $\mathcal{O}_2$ essentially isolate the same region and there is no special advantage in selecting one over the other. In light of the investiations above, the constraints from the two CT points give the following ranges for the scalar radius and the curvature parameters: if the ratio of F_K/F_π is fixed to be 1.21, then varying the value of the scalar form factor at the second CT point by about 3% from its one-loop value leads to the ranges $0.12\,\mathrm{fm}^2 \lesssim \langle r^2\rangle_S^{K\pi} \lesssim 0.21\,\mathrm{fm}^2$ and $0.56\,\mathrm{GeV}^{-4} \lesssim c \lesssim 1.47\,\mathrm{GeV}^{-4}$ and it may be observed that there is a strong correlation between the two given by our ellipses. On the other hand, if the ratio of the decay constants is somewhat lower, then the ellipses migrate to the left. Note that this determination of the radius gives for the slope parameter $\lambda_0 (\equiv \langle r^2\rangle_S^{K\pi} m_\pi^2/6)$ the range $10\times10^{-3} \lesssim \lambda_0 \lesssim 17\times10^{-3}$ (for a discussion of present-day experimental status see ref. [1]). Finally, the following may be noted: the inclusion of the phase of the form factor with i) the datum from the second CT point, or ii) extending the framework of BC further to include the data from both CT points are worth studying. The analysis also may shed light on issues considered in many recent studies, *e.g.*, refs. [9,20]. Indeed, BC have constrained the constants C_{12}^r and C_{34}^r; our results could also be extended to meet such an end. While our work points to a correction of about −3% to the one-loop value of the scalar form factor due to higher-order effects at the second CT point, an interesting analysis would be one that parallels, *e.g.*, ref. [5] using more current values of F_K/F_π.

BA thanks DST for support. We are indebted to I. Caprini and H. Leutwyler for detailed comments on the manuscript, J. Bijnens, B. Moussallam and E. Passemar for correspondence and S. Ramanan for discussions.

Appendix A.

In this appendix, we list the relevant outer functions:

$$w_{\mathcal{O}_1} = \frac{1}{4}\sqrt{\frac{3}{2\pi}} \times\frac{m_K - m_\pi}{m_K + m_\pi}\,\frac{(1-z)(1+z)^{3/2}\sqrt{1-z+\beta(1+z)}}{(1-z+\beta_Q(1+z))^3},$$

$$w_{\mathcal{O}_2} = w_{\mathcal{O}_1} \times \frac{1-z+\beta_Q(1+z)}{\sqrt{8}}$$

and

$$w_{\mathcal{O}_3} = \frac{(1-d)^2}{32t_+(1-z_-)^{5/2}}\sqrt{\frac{3}{4\pi t_+}}\,\frac{(1+z)(1-z)^{5/2}}{(1-zz_-)^{1/4}(1-zd)^2},$$

with

$$\beta = \sqrt{1-t_-/t_+}, \qquad t_- = (m_K - m_\pi)^2,$$

$$\beta_Q = \sqrt{1+Q^2/t_+},$$

$$d = \left(\sqrt{t_+ + Q^2} - \sqrt{t_+}\right) \Big/ \left(\sqrt{t_+ + Q^2} + \sqrt{t_+}\right) \quad \text{and}$$

$$z_- = \left(\sqrt{t_+ - t_-} - \sqrt{t_+}\right) \Big/ \left(\sqrt{t_+ - t_-} + \sqrt{t_+}\right).$$

References

1. FlaviaNet Working Group on Kaon Decays (M. Antonelli *et al.*), arXiv:0801.1817 [hep-ph].
2. J. Gasser, H. Leutwyler, Nucl. Phys. B **250**, 517 (1985).
3. P. Post, K. Schilcher, Eur. Phys. J. C **25**, 427 (2002) (arXiv:hep-ph/0112352).
4. J. Bijnens, P. Talavera, Nucl. Phys. B **669**, 341 (2003) (arXiv:hep-ph/0303103).
5. M. Jamin, J.A. Oller, A. Pich, JHEP **0402**, 047 (2004) (arXiv:hep-ph/0401080).
6. C.G. Callan, S.B. Treiman, Phys. Rev. Lett. **16**, 153 (1966).
7. R.F. Dashen, M. Weinstein, Phys. Rev. Lett. **22**, 1337 (1969).
8. J. Bijnens, K. Ghorbani, arXiv:0711.0148 [hep-ph].
9. A. Kastner, H. Neufeld, Eur. Phys. J. C **57**, 541 (2008) (arXiv:0805.2222 [hep-ph]).
10. V. Cirigliano, G. Ecker, M. Eidemuller, R. Kaiser, A. Pich, J. Portoles, JHEP **0504**, 006 (2005) (arXiv:hep-ph/0503108).
11. V. Bernard, M. Oertel, E. Passemar, J. Stern, arXiv:0903.1654 [hep-ph].
12. R. Oheme, Phys. Rev. Lett. **16**, 215 (1966).
13. C. Bourrely, I. Caprini, Nucl. Phys. B **722**, 149 (2005) (arXiv:hep-ph/0504016).

14. C. Bourrely, B. Machet, E. de Rafael, Nucl. Phys. B **189**, 157 (1981).
15. I. Caprini, Eur. Phys. J. C **13**, 471 (2000) (arXiv:hep-ph/9907227).
16. B. Ananthanarayan, S. Ramanan, Eur. Phys. J. C **54**, 461 (2008) (arXiv:0801.2023 [hep-ph]).
17. HPQCD Collaboration and MILC Collaboration and UKQCD Collaboration (C. Aubin *et al.*), Phys. Rev. D **70**, 031504 (2004) (arXiv:hep-lat/0405022).
18. QCDSF Collaboration and UKQCD Collaboration (M. Gockeler, R. Horsley, A.C. Irving, D. Pleiter, P.E.L. Rakow, G. Schierholz, H. Stuben), Phys. Lett. B **639**, 307 (2006) (arXiv:hep-ph/0409312).
19. European Twisted Mass Collaboration (B. Blossier *et al.*), JHEP **0804**, 020 (2008) (arXiv:0709.4574 [hep-lat]).
20. V. Bernard, M. Oertel, E. Passemar, J. Stern, JHEP **0801**, 015 (2008) (arXiv:0707.4194 [hep-ph]).